Triple-Resonance ^{1}H–^{19}F–^{13}C CPMAS NMR Study on the Crystallization Behavior of the PMMA/PVF_2 60/40 Blend

C. H. M. Papavoine, W. E. J. R. Maas,† and W. S. Veeman*,‡

Nijmegen SON Research Center for Molecular Structure, Design and Synthesis, Department of Molecular Spectroscopy, University of Nijmegen, 6525 ED Nijmegen, The Netherlands

G. H. Werumeus Buning

DSM Research, Department CP-NK, P.O. Box 18, 1660 MD Geleen, The Netherlands

J. M. J. Vankan

Philips Research Laboratories, P.O. Box 80.000, 5600 JA Eindhoven, The Netherlands

Received November 2, 1992; Revised Manuscript Received July 19, 1993•

ABSTRACT: We introduce a new approach to study phase separation phenomena in polymer blends. The crystallization of PVF_2 in a 60/40 blend of poly(methyl methacrylate) (PMMA) and poly(vinylidene fluoride) (PVF_2) is investigated using triple-resonance ^{1}H–^{13}C–^{19}F cross polarization magic angle spinning nuclear magnetic resonance (CPMAS NMR). This technique enables the determination of the fractions of PMMA and PVF_2 that are not mixed at a molecular scale. Differential scanning calorimetry (DSC) measurements are performed which give information about the degree of crystallinity in the blend. The presence of an amorphous PVF_2 interphase has been found, confirming recent studies on the existence of such an interphase upon crystallization. The different crystallization behavior between the 60/40 PMMA/PVF_2 blend annealed at 120 °C and the blend annealed at 140 °C suggests the existence of an upper critical solution temperature for this system.

1. Introduction

Poly(methyl methacrylate) (PMMA) and poly(vinylidene fluoride) (PVF_2) form a miscible blend, which is completely amorphous when quenched from the melt.[1] Despite the favorable interactions between PMMA and PVF_2 segments, which lead to a negative value for the Flory–Huggins interaction parameter, PVF_2 can partially crystallize in the blend. Upon crystallization of PVF_2 it is believed that a triphasic system is formed, consisting of PVF_2 crystallites, an amorphous PMMA/PVF_2 phase, and an amorphous PVF_2 interphase surrounding the crystallites.[2]

The crystallization of PVF_2 in its blends with PMMA has been the subject of a number of papers. Some of these papers deal with the depression of the melting point of PVF_2 crystals upon blending with PMMA,[1,3–5] in order to obtain information on the miscibility of the components. Other studies pay attention to morphology and to the kinetics of the crystal growth.[2,6–9]

In this report we introduce a new approach to study phase separation at a molecular scale in polymer blends. We show the applicability of solid-state NMR to the study of phase separation in the PMMA/PVF_2 blend upon annealing above T_g. We employ the ^{1}H–^{19}F cross depolarization technique, which has previously been introduced[10] and has proven to be sensitive to the local environments of PMMA and PVF_2 segments.[10,11] Before presenting the results of these experiments on annealed PMMA/PVF_2 samples, we will briefly review the cross depolarization experiment.

2. Experimental Section

A. Blend. The atactic PMMA used was PMMA 6 N from Röhm GMBH (Darmstadt). This polymer contains 10% methyl acrylate groups. Its average molecular weight $\bar{M}_w$, determined with GPC relative to polystyrene standards, was 100 000 g/mol. The T_g of the material was 379 K (DSC, heating rate 20 K/min). The PVF_2 used was Kynar homopolymer-grade 401 with an average molecular weight $\bar{M}_w$ of 530 000 g/mol (Pennwalt) and a T_g of 243 K. Blends were prepared via coprecipitation and subsequent compression molding, as described by Roerdink and Challa.[4] For a PMMA/PVF_2 60/40 weight ratio of the blend, 7.5 g of the mixture was dissolved in 250 g of DMF (Merck). The solution was added dropwise to 3 L of water. The precipitated mixture was filtered off and dried at high vacuum for a minimum of 6 days at 50 °C and for several hours at 160 °C to remove the last traces of solvent. The dried mixture was then molded in a press at 200 °C prior to quenching from the melt in liquid nitrogen.

B. NMR Data. Experiments were performed on a Bruker CXP 300 spectrometer, operating at 300.1, 282.2, and 75.4 MHz for ^{1}H, ^{19}F, and ^{13}C NMR, respectively. A standard Bruker double-bearing MAS probehead was used. The triple tuning of the probehead was achieved by using a previously described setup.[12] Magic angle spinning rates were 3.5 kHz. RF field strengths were typically 50 kHz on protons, fluorines, and carbon. Carbon free induction decays were acquired under simultaneous proton and fluorine high-power decoupling. In experiments involving cross polarization, spin temperature alternation was used. All experiments were performed at room temperature. Figure 1 shows the pulse scheme for the ^{1}H–^{19}F cross depolarization experiment. A $\pi/2$ pulse at the ^{1}H frequency is applied prior to a Hartmann–Hahn matched spin-lock on ^{1}H and ^{19}F during a variable time t, in which protons can lose their magnetization to the fluorines. Subsequently, the remaining proton magnetization is transferred to carbons via ^{1}H–^{13}C cross polarization during 1 ms and the carbon magnetization is detected. To prevent fluorine magnetization from building up during the first step of the experiment, the phase of the fluorine RF field is shifted every 50 μs.

C. Annealing. The samples were placed in an oven at either 120 or 140 °C for a certain time t_{ann}. The temperature was controlled within ±2 K. After the treatment of NMR samples were quenched in liquid nitrogen. The glass transition temper-

* To whom correspondence should be addressed.
† Present address: Bruker Instruments Inc., Fortune Drive, Billerica, MA 01821.
‡ Present address: Physikalische Chemie, Fachbereich 6, Universität-GH-Duisburg, Lotharstrasse 1, 4100 Duisburg 1, Germany.
• Abstract published in *Advance ACS Abstracts*, October 15, 1993.

0024-9297/93/2226-6611$04.00/0

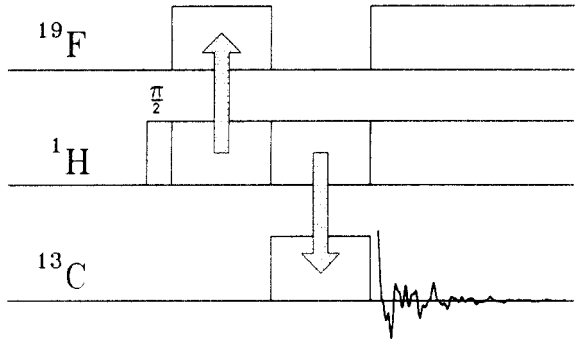

Figure 1. Pulse sequence of the ^1H–^{19}F cross depolarization experiment with ^{13}C detection. The heavy arrows indicate the polarization transfer. Variation of the ^1H–^{19}F contact time enables the determination of the isolated PMMA and PVF_2 fractions.

ature, T_g, and the crystalline PVF_2 fraction of the annealed blends and the melting temperature T_m were determined using a Perkin-Elmer differential scanning calorimeter. The heating rate was 10 K/min. The annealed samples were subjected to a ^1H–^{19}F cross depolarization experiment.

3. ^1H–^{19}F Cross Depolarization

The ^1H–^{19}F cross depolarization technique discriminates between PMMA and PVF_2 segments that are close to or remote from each other, based on whether the distance between the segments can or cannot be bridged by proton spin diffusion. The experiment starts by creating spin-locked proton magnetization in the whole sample. Subsequently, a fluorine RF field is applied whose strength fulfills the proton–fluorine Hartmann–Hahn condition. Protons that are dipolarly coupled to fluorine spins will then transfer their magnetization to the fluorines. The fluorine reservoir acts as a sink in which proton magnetization can disappear. If the fluorine RF field is turned off, only proton magnetization remains from protons that do not have a dipolar coupling with fluorines and thus are remote from fluorines. An additional feature in this experiment is the occurrence of proton spin diffusion. As soon as proton magnetization is destroyed in a region close to fluorines, then proton magnetization will be transported toward this region, driven by the magnetization gradient.

After the fluorine RF field is turned off, the leftover proton magnetization is transferred to carbons via ^1H–^{13}C cross polarization, and the carbon free induction decay is acquired under simultaneous proton and fluorine high-power decoupling. This enables us to monitor the PMMA and PVF_2 carbon resonances separately (see Figure 2) and as a function of the ^1H–^{19}F cross depolarization time.

Apart from possible losses to the fluorine sink, spin-locked proton magnetization will be lost to the lattice through $T_{1\rho}$ relaxation. The carbon intensities as a function of the ^1H–^{19}F cross depolarization time are corrected for losses due to ^1H–$T_{1\rho}$ relaxation by dividing these values by the intensities obtained from a blank experiment.[10] In this blank experiment no fluorine RF field is used, and the loss of proton polarization is entirely due to $T_{1\rho}$ relaxation. We will discuss this in more detail below, but in representing the data in this manner it is assured that the disappearance of proton magnetization is due solely to the cross depolarization process, regardless of local variations in proton $T_{1\rho}$ values.

In a previous publication[10] we have analyzed the results of ^1H–^{19}F cross depolarization experiments on PMMA/PVF_2 using a four-phase model for the blend. This model proved adequate to explain the experimental data and to detect differences between blends with different weight

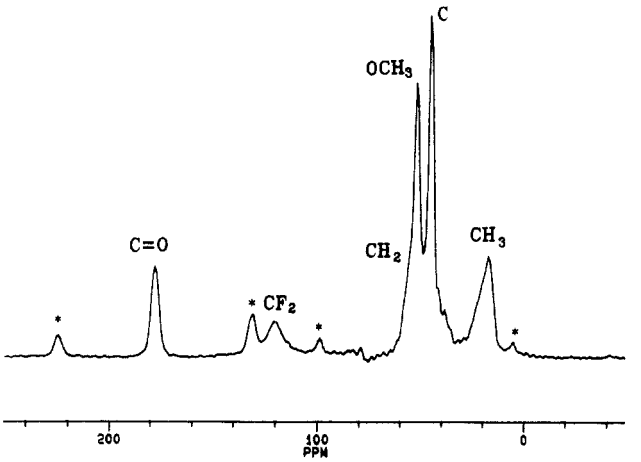

Figure 2. ^{13}C CPMAS NMR spectrum of the PMMA/PVF_2 60/40 blend, obtained with simultaneous ^1H and ^{19}F high-power decoupling. The carbon resonances are assigned; the CH_2 of PVF_2 overlaps with the quaternary ^{13}C resonance of PMMA. The spinning sidebands are marked with an asterisk.

ratios[10] and between blends with varying PMMA tacticity.[11] The focus of this study is somewhat different in that we want to examine the changes induced in PMMA/PVF_2 blends upon annealing. In order to observe the expected phase separation phenomena, we only need to determine the amounts of PMMA and PVF_2 that are close to or remote from each other. We define the fraction of PMMA that is not affected by the cross depolarization experiment as the isolated PMMA fraction. The carbon signal intensities of this fraction will remain constant as a function of time in the experiment, since no proton magnetization is transferred to the fluorine sink. Similarly, we define an isolated PVF_2 fraction as the amount of PVF_2 in the blend whose protons lose magnetization to the fluorines at a rate (T_{HF}^{-1}) which is equal to that observed in pure PVF_2. Clearly, the PVF_2 proton magnetization in this fraction is not affected by magnetization transfer from PMMA protons because the distance between this isolated PVF_2 region and PMMA regions is too large to be bridged by spin diffusion.

As has been described in detailed by Maas et al.,[10] both the isolated PMMA and PVF_2 fractions can be determined without assuming a specific model for the spatial distribution in the blend. We define the fractions of PVF_2 and PMMA that are affected by the cross depolarization as the mixed fractions f_{mix}. If we denote the PMMA signal from the depolarization experiment S_1, and the signal from the blank experiment S_2, we can write the observed signals as

$$S_1(t) = S_0 f_{mix} \exp\left(\frac{-t}{T_{1\rho}}\right) D(t) + S_0(1 - f_{mix}) \exp\left(\frac{-t}{T_{1\rho}}\right) \quad (1)$$

$$S_2(t) = (S_0 f_{mix} + S_0(1 - f_{mix})) \exp\left(\frac{-t}{T_{1\rho}}\right) \quad (2)$$

where S_0 is the total proton magnetization, f_{mix} is the fraction of protons close to fluorines, $D(t)$ is a decaying function which describes the loss of magnetization due to depolarization to the fluorine sink, and t is the cross depolarization time. By dividing both signals, we have corrected for loss of magnetization to the lattice, characterized by the proton $T_{1\rho}$

$$S(t) = \frac{S_1(t)}{S_2(t)} = f_{mix} D(t) + (1 - f_{mix}) \quad (3)$$

where $S(t)$ is the proton $T_{1\rho}$ corrected cross depolarization

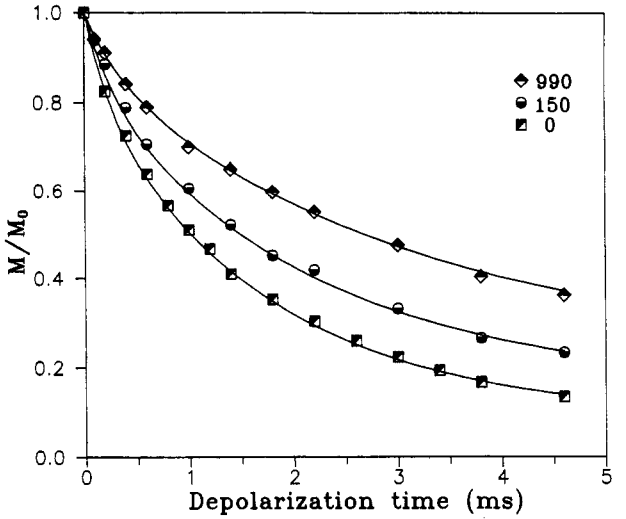

Figure 3. OCH_3 carbon intensities as a function of the cross depolarization time for blends annealed at 140 °C for 0, 150, and 990 min. The intensities are scaled with respect to the intensity at zero depolarization time (M/M_0).

intensity at time t. A similar reasoning follows for the PVF_2 proton magnetization. Since the results from two experiments are divided, instead of a division by an average value for the proton $T_{1\rho}$, the correction is independent of local variations in proton $T_{1\rho}$'s.

The PMMA ($S^M(t)$) and PVF_2 ($S^V(t)$) carbon intensities as a function of the ^1H–^{19}F cross depolarization time t and corrected for ^1H–$T_{1\rho}$ relaxation can thus be equated as

$$S^M(t) = f^M_{mix}D(t) + (1 - f^M_{mix}) \quad (4)$$

$$S^V(t) = f^V_{mix}D(t) + (1 - f^V_{mix}) \exp\left(\frac{-t}{T_{HF}}\right) \quad (5)$$

where f^M_{mix} and f^V_{mix} are the mixed PMMA and PVF_2 fractions, respectively, $(1 - f^M_{mix})$ and $(1 - f^V_{mix})$ are the isolated fractions of PMMA and PVF_2, respectively, and $D(t)$ is a function which decays to zero and which describes the loss of proton magnetization to the sink through ^1H–^{19}F cross depolarization and proton spin diffusion. The equations for PMMA and PVF_2 differ in an extra term $\exp(-t/T_{HF})$ which arises from the fact that protons from isolated PVF_2 still lose their magnetization to the fluorine sink since all PVF_2 protons are close to fluorines.

We will abstain from a discussion on the specific form of $D(t)$ in this publication and use the above given equations only to determine the isolated fractions, using the fact that $D(t)$ decays to zero for long values of t.

4. Results

PMMA/PVF_2 60/40 samples are annealed in an oven at either 120 to 140 °C for an annealing time t_{ann}, after which the samples are quenched in liquid nitrogen and a ^1H–^{19}F cross depolarization experiment is performed. Upon annealing, phase separation takes place in the blend, which shows from the experiments by an increase in the fractions of isolated PMMA and PVF_2. Some examples of depolarization curves are shown in Figure 3 for the PMMA OCH_3 carbon resonance of a blend, annealed at 140 °C for 0, 150, and 990 min. A similar behavior is observed for the blend annealed at 120 °C. In Figures 4 and 5 the fractions isolated PMMA and PVF_2 are plotted as a function of the annealing time and at different temperatures. In addition to these data, it was found that the proton $T_{1\rho}$ values gradually increased with longer annealing times.

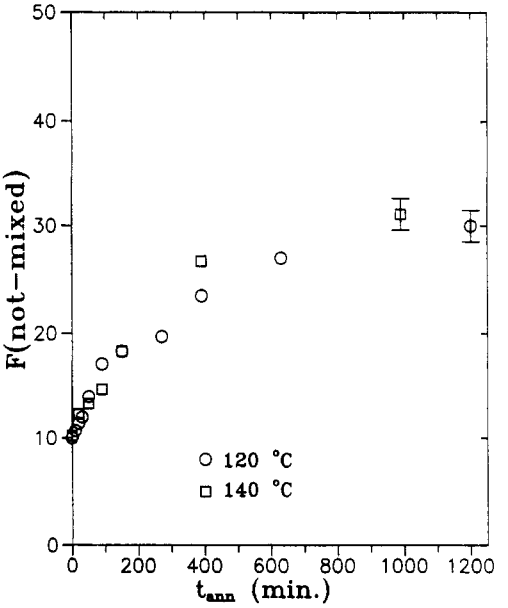

Figure 4. Fractions of isolated PMMA, as a function of the annealing time at 120 and 140 °C.

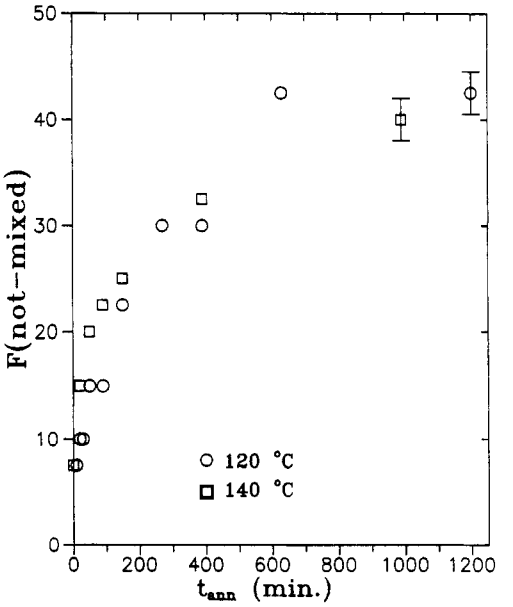

Figure 5. Fractions of isolated PVF_2, as a function of the annealing time at 120 and 140 °C.

Since the isolated fractions of PMMA and PVF_2 are determined, the fractions of PMMA and PVF_2 that are close to each other are also known. If we define these fractions as the fractions in the mixed region, then it is possible to calculate the monomer ratio of PMMA and PVF_2 in this region. The monomer ratio in the whole sample can be calculated from the PMMA/PVF_2 weight ratio using a molecular weight for a MMA monomer of 100 and for a VF_2 monomer of 64. If we subtract from this the fractions of PMMA and PVF_2 that are not mixed, we obtain the monomer ratio in the mixed region. The monomer ratios (MR) of the blend annealed at 120 and 140 °C are listed in Table I as a function of the annealing time.

In another experiment, the blend annealed at 140 °C for 990 min was heated in an oven at 190 °C, which is well above the melting temperature of the PVF_2 crystals in the blend. After a certain time, the sample was quenched in liquid nitrogen, and a cross depolarization experiment was performed. It appeared that after only 10 min at 190 °C all the PMMA and PVF_2 were mixed again (see Figure 6),

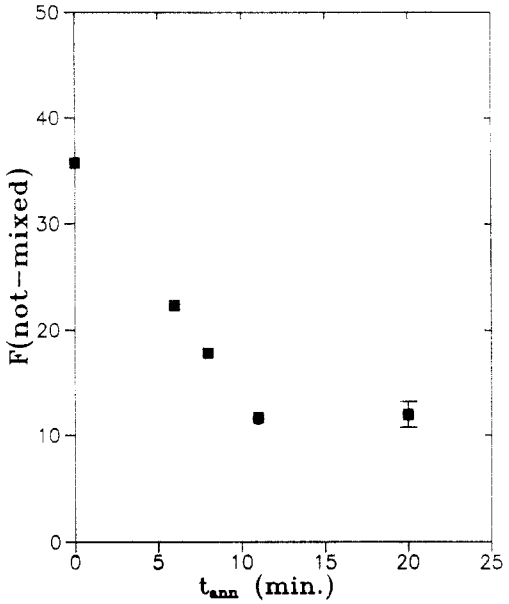

Figure 6. Fraction of isolated PMMA as a function of the annealing time at 190 °C for a sample first annealed for 990 min at 140 °C.

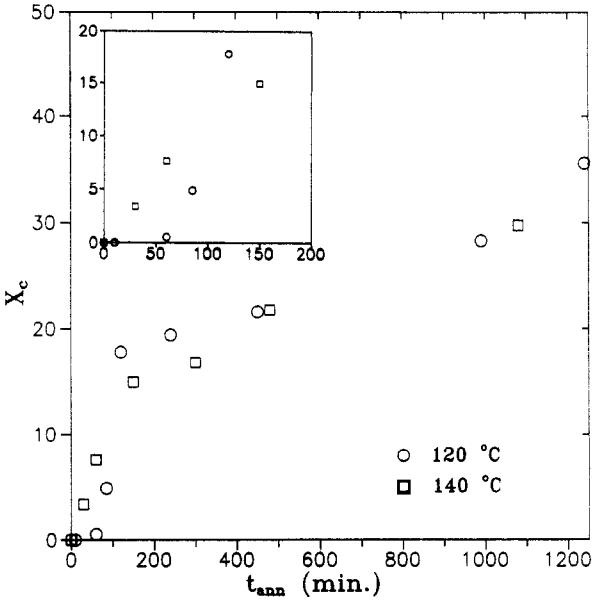

Figure 7. Crystalline fraction of PVF_2, determined with DSC, as a function of the annealing time at 120 and 140 °C. The insert shows the short time behavior.

Table I. Monomer Ratios (MR) PMMA/PVF_2 in the Mixed Region of the PMMA/PVF_2 60/50 Blends, Annealed at 120 and 140 °C

t_{ann} (min)	MR 120 °C	MR 140 °C
0	0.93	0.93
20	0.95	0.99
50	0.97	1.04
90	0.97	1.07
150	1.01	1.05
390	1.05	1.04
630	1.17	
990		1.10
1200	1.17	

Table II. Glass Transition Temperatures T_g of the PMMA/PVF_2 60/40 Blends, Annealed at 120 and 140 °C

t_{ann} (min)	T_g (K) 120 °C	T_g (K) 140 °C
0	336	336
60	337	341
120	344	
240	347	
300		342
450	346	
480		345
990	350	
1080		349
1240	351	

which means that the fractions of isolated PMMA and PVF_2 are again at the same values as before annealing. Melting at 190 °C for longer times did not decrease these values.

In addition to the NMR experiments DSC measurements are performed. Upon annealing, the DSC spectra show a melting peak from PVF_2 crystallites, which enables the determination of the degree of crystallinity in the samples.[13] Figure 7 shows the degree of crystallinity X_c as a function of the annealing time and temperature. The values of X_c are ratios of the specific enthalpies of fusion of PVF_2 in the blend and in the homopolymer (25 cal g^{-1}).[13] From the DSC measurements we also obtained the glass transition temperature of the blend. These T_g's are listed in Table II for annealing at 120 and 140 °C and shifted to higher values as a function of the annealing time.

5. Discussion

The isolated fractions of PMMA and PVF_2 in the PMMA/PVF_2 60/40 blend before annealing are very small, 10% and 7%, respectively, indicating that PMMA and PVF_2 are miscible at a molecular scale. Also, the observation of a single proton $T_{1\rho}$ for this blend shows that the amounts of PMMA and PVF_2 that are not intimately mixed do not form large separate domains, but are apparently in between regions of intimately mixed material. On the basis of previous studies,[10,11] we believe that a separation on the order of 2–3 nm qualifies polymer segments to be regarded as isolated in the cross depolarization experiment.

The cross depolarization experiments as a function of the annealing time at either 120 or 140 °C show that phase separation occurs in the PMMA/PVF_2 blend upon annealing. Both the isolated PMMA and PVF_2 fractions increase, which indicates a displacement of polymer segments at these temperatures, such that the distance between these fractions is too large for both proton–fluorine and proton–proton magnetization transfer. From DSC experiments it is concluded that at least a part of the increase in the fraction of unmixed PVF_2, observed in the NMR experiments, is due to crystallization of PVF_2 in the blend.

PVF_2 is known to exist in a variety of crystal forms. Leonard et al.[6] showed that under these annealing conditions PVF_2 in the PMMA/PVF_2 60/40 blend crystallizes in the α-modification. From NMR and DSC data it is found that both the increase in the isolated PVF_2 fraction and the increase in the crystalline fraction slow down at longer annealing times. Wang and Nishi[9] reported constant radial growth rates of PVF_2 spherulites in PMMA/PVF_2 blends (although with higher PVF_2 content), which is not supported by either our NMR or our DSC data. However, their measurements cover only a small time period relative to the growth rate, and constant growth rates can be observed at short annealing times (see Figures 5 and 7). Morra and Stein[14,15] pointed out that the growth rate should continuously decrease, due to depletion of PVF_2 in the amorphous regions surrounding the crystals. Since the crystal growth front only uses PVF_2 chains as the crystal grows, a PMMA richer phase is formed at the outer surface, retarding the crystal growth. This explains the trends in our data with increasing annealing time.

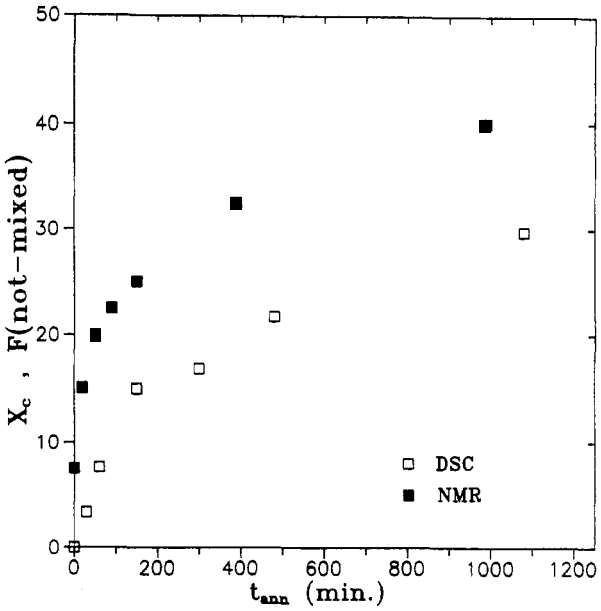

Figure 8. Comparison of the crystalline fraction determined by DSC and the isolated fraction determined by NMR of PVF_2 as a function of the annealing time at 140 °C.

Evidence for a PMMA-richer phase, due to depletion of PVF_2 in the mixed region, was also found by Tékély et al., who observed an increase in proton $T_{1\rho}$ values in a PMMA/PVF_2 50/50 blend as a function of the annealing time. In a well-mixed blend, the observed proton $T_{1\rho}$'s are averaged by proton spin diffusion and found to be in between the $T_{1\rho}$'s of the homopolymers. From our experiments we find an increase of the PMMA/PVF_2 monomer ratio in the mixed phase, of the proton $T_{1\rho}$ and of the T_g of the blend, with increasing annealing time. These results are all indicative of an increasing PMMA content in the amorphous phase.

There is a significant discrepancy between the fraction of crystalline PVF_2, obtained from the DSC experiments, and the fraction of unmixed PVF_2, obtained from the NMR experiments (see Figure 8). Hahn et al.[2,16] suggest the existence of a crystal–amorphous PVF_2-interphase. This interphase is believed to be caused by head-to-head and tail-to-tail defects in PVF_2 and is expected to expel PMMA. Since the difference between the NMR and DSC data (Figure 8) approaches a constant value after an initial annealing time, we believe that our data support the suggestion of a crystal–amorphous PVF_2-interphase. In a previous study we have utilized the ^1H–^{19}F cross depolarization technique to study PMMA/PVF_2 blends with varying composition.[10] It was shown that in unannealed PMMA/PVF_2 blends the fraction of unmixed PMMA increases with increasing PMMA content, while the fraction of unmixed PVF_2 decreases with higher PMMA/PVF_2 ratio. Here, we observe that the unmixed PMMA fraction increases as a function of the annealing time and also that the fraction of unmixed PVF_2 increases. Moreover, this increase is larger than what can be accounted for by a PVF_2 crystalline fraction, so the existence of an amorphous PVF_2 interphase seems likely. Also, if PMMA would be present next to PVF_2 crystallites, one would expect either some direct proton to fluorine magnetization transfer or proton spin diffusion from PMMA to, at least, the outer regions of the PVF_2 crystallites. In that case segments on the outside of the crystallites would still be regarded as mixed in the cross depolarization experiment. This would result in a lower fraction of isolated PVF_2 from the NMR experiments compared to the crystalline fraction found from the DSC experiments, and this is contrary to the experimental results.

From the NMR data, after melting at 190 °C (Figure 6), we observe that the crystals have melted and are intimately mixed again after approximately 10 min. This means that no large PVF_2 spherulites have developed upon annealing. The remixing of PVF_2 and PMMA after melting of the PVF_2 crystals is governed by diffusion. If we approximate the mean displacement[17] of the polymer chains by $d = (2Dt)^{1/2}$ and use the diffusion coefficient of PVF_2, which is $\approx 10^{-10}$ cm^2 s^{-1} at 190 °C,[18,19] this would pose an upper limit on the radii of the crystallites of approximately 3.5 μm. Due to the depletion of PVF_2 in the amorphous region surrounding the crystals, the crystal growth is hindered, which may cause new nucleation events to occur before the crystals can grow large and may lead to the formation of many small crystals.

Finally, we briefly comment on the differences observed at short annealing times for different annealing temperatures. The crystalline fractions, obtained from DSC experiments of blends annealed at 120 °C (see Figure 7), abruptly increase only after a certain annealing time. The NMR data however (Figure 5) show an immediate increase in the amount of unmixed PVF_2 with annealing time. These differences are not observed for the blends annealed at 140 °C. The difference may be caused by a failure of DSC to detect small amounts of crystallinity. However, Saito et al.[7] reported convincing evidence of upper critical solution temperature (UCST) behavior in PMMA/PVF_2 blends. For the PMMA/PVF_2 60/40 blend the UCST was determined at approximately 120 °C. This means that below this temperature the observed phase separation is due to spinodal decomposition, whose rate prevails over that of crystallization. Although our data are not conclusive, the possibility of an UCST, located in between 120 and 140 °C, cannot be ruled out. In view of this we also mention a study by Grinsted and Koenig,[20] who reported separation between unlike chains in PMMA/PVF_2 samples after aging of 2 months at room temperature. It may well be that spinodal decomposition is responsible for this behavior.

6. Conclusions

We have introduced a new approach to study phase separation in polymer blends. The phase separation of a PMMA/PVF_2 60/40 blend upon annealing is investigated with ^1H–^{19}F cross depolarization solid-state NMR. This experiment yields information on the fractions of PVF_2 and PMMA that are intimately mixed and enables us to monitor these fractions as a function of the annealing time. The cross depolarization experiment is sensitive to small sparations between polymer domains, on the order of 2–3 nm, and therefore provides unique information on miscibility at a molecular scale. The observed phase separation is induced by crystallization of PVF_2 in the blend. In comparing the NMR data with DSC data the existence of an amorphous PVF_2 phase in the blend is shown, which is in agreement with studies by Hahn et al.[2] The observed differences in phase separation between samples annealed at 120 and 140 °C suggest the existence of an UCST for this system.

The crystallization of PVF_2 in PMMA/PVF_2 blends is a complex process, which is influenced by many parameters, both from thermodynamic and kinetic origin. The results presented in this paper demonstrate that the ^1H–^{19}F cross depolarization experiment can be a useful tool for the study of phase separation phenomena.

Acknowledgment. This work was supported by the Dutch Research Foundation (NWO/SON). We thank Mr. J. W. M. van Os, Mr. A. A. G. van Oijen, Mr. G. W. J. Janssen, and Mrs. G. H. Nachtegaal for technical assistance at the Dutch National NMR Facility at Nijmegen.

References and Notes

(1) Léonard, C.; Halary, J. L.; Monnerie, L. *Macromolecules* **1988**, *21*, 2988.
(2) Hahn, B. R.; Hermann-Schonherr, O.; Wendorff, J. H. *Polymer* **1987**, *28*, 201.
(3) Nishi, T.; Wang, T. T. *Macromolecules* **1975**, *8*, 909.
(4) Roerdink, E.; Challa, G. *Polymer* **1978**, *19*, 173.
(5) Chow, T. S. *Macromolecules* **1990**, *23*, 333.
(6) Léonard, C.; Halary, J. L.; Monnerie, L.; Broussoux, D.; Servet, B.; Micheron, F. *Polym. Commun.* **1983**, *24*, 110.
(7) Saito, H.; Fujita, Y.; Inoue, T. *Polym. J.* **1987**, *19*, 405.
(8) Tékély, P.; Lauprêtre, F.; Monnerie, L. *Polymer* **1985**, *26*, 1081.
(9) Wang, T. T.; Nishi, T. *Macromolecules* **1977**, *10*, 421.
(10) Maas, W. E. J. R.; van der Heijden, W. A. C.; Veeman, W. S.; Vankan, J. M. J.; Werumeus Buning, G. H. *J. Chem. Phys.* **1991**, *95*, 4698.
(11) Eijkelenboom, A.; Mass, W. E. J. R.; Veeman, W. S.; Vankan, J. M. J.; Werumeus Buning, G. H. *Macromolecules* **1992**, *25*, 18.
(12) Klein Douwel, C. H.; Maas, W. E. J. R.; Veeman, W. S.; Werumeus Buning, G. H.; Vankan, J. M. J. *Macromolecules* **1990**, *23*, 406.
(13) Nakagawa, K.; Ishida, Y. *Polym. Sci.* **1973**, *11*, 2153.
(14) Morra, B. S.; Stein, R. S. *J. Polym. Sci., Polym. Phys. Ed.* **1982**, *20*, 2261.
(15) Morra, B. S.; Stein, R. S. *Polym. Eng. Sci.* **1984**, *24*, 311.
(16) Hahn, B.; Wendorff, J., Yoon, D. Y. *Macromolecules* **1985**, *18*, 718.
(17) Crank, J. *The Mathematics of Diffusion*; Oxford University Press: Oxford, 1957.
(18) Maas, W. E. J. R.; Papavoine, C. H. M.; Veeman, W. S.; Vankan, J. M. J.; Werumeus Buning, G. H. Submitted for publication.
(19) Wu, S.; Chuang, H. K.; Han, C. D. *J. Polym. Sci., Polym. Phys. Ed.* **1986**, *24*, 143.
(20) Grinsted, R. A.; Koenig, J. L. *J. Polym. Sci., Polym. Phys. Ed.* **1990**, *28*, 177.